Nutrient and salinity decadal variations in the central and eastern North Pacific

E. Di Lorenzo,[1] J. Fiechter,[2] N. Schneider,[3] A. Bracco,[1] A. J. Miller,[4] P. J. S. Franks,[4] S. J. Bograd,[5] A. M. Moore,[2] A. C. Thomas,[6] W. Crawford,[7] A. Peña,[7] and A. J. Hermann[8]

Received 7 April 2009; revised 7 May 2009; accepted 14 May 2009; published 16 July 2009.

[1] Long-term timeseries of upper ocean salinity and nutrients collected in the Alaskan Gyre along Line P exhibit significant decadal variations that are shown to be in phase with variations recorded in the Southern California Current System by the California Cooperative Oceanic Fisheries Investigation (CalCOFI). We present evidence that these variations are linked to the North Pacific Gyre Oscillation (NPGO)—a climate mode of variability that tracks changes in strength of the central and eastern branches of the North Pacific gyres and of the Kuroshio-Oyashio Extension (KOE). The NPGO emerges as the leading mode of low-frequency variability for salinity and nutrients. We reconstruct the spatial expressions of the salinity and nutrient modes over the northeast Pacific using a regional ocean model hindcast from 1963-2004. These modes exhibit a large-scale coherent pattern that predicts the in-phase relationship between the Alaskan Gyre and California Current timeseries. The fact that large-amplitude, low-frequency fluctuations in salinity and nutrients are spatially phase-locked and correlated with a measurable climate index (the NPGO) open new avenues for exploring and predicting the effects of long-term climate change on marine ecosystem dynamics. **Citation:** Di Lorenzo, E., et al. (2009), Nutrient and salinity decadal variations in the central and eastern North Pacific, *Geophys. Res. Lett.*, *36*, L14601, doi:10.1029/2009GL038261.

1. Introduction

[2] For over half a century the CalCOFI and Line P observational programs have routinely collected observations of upper ocean physical, chemical and biological properties in the northeast Pacific [*Crawford et al.*, 2007; *Freeland*, 2007; *Peña and Bograd*, 2007; *Peña and Varela*, 2007]. Although temperature observations have been widely collected in other regions of the North Pacific, sustained timeseries of salinity and nutrients such as those at Line P and CalCOFI are rare. The lack of long-term records of salinity and nutrient has led to an incomplete view of the mechanisms controlling the physical, chemical and biological ocean climate of the North Pacific. Analysis of sea surface temperature anomalies (SSTa) in the North Pacific have isolated the Pacific Decadal Oscillation (PDO) as the dominant mode of SSTa variability [*Mantua et al.*, 1997]. The PDO exhibits strong decadal fluctuations and regime-like behaviors (e.g., observed shift in 1976–77) that have been invoked to explain part of the variability of physical and biological properties across the North Pacific [*McGowan et al.*, 2003]. However, the PDO fails to capture the prominent low-frequency fluctuations in salinity and nutrients recorded in the California Current System (CCS) [*Di Lorenzo et al.*, 2008] and in the Gulf of Alaska (GoA) Line P timeseries. In the CCS, it has been shown that surface salinity and subsurface nutrient variability are correlated with the North Pacific Gyre Oscillation (NPGO) [*Di Lorenzo et al.*, 2008], a mode of decadal climate variability defined as the second dominant mode of sea-surface height anomaly (SSHa) variability in the northeast Pacific over the region 180°–110°W; 25°N–62°N. Non-seasonal salinity and nutrient fluctuations exert important controls on the productivity of lower trophic levels of marine food webs. The extent to which these fluctuations in the CCS co-vary with those in the GoA, thereby defining coherent ecosystem variability across the whole central and eastern North Pacific, remains unknown.

[3] Physically the NPGO captures changes in strength of the North Pacific Current (NPC) [*Di Lorenzo et al.*, 2008] and of the Kuroshio-Oyashio Extension (KOE) [*Ceballos et al.*, 2009] (Figure 1), which mark the boundary between the subpolar and subtropical gyres. This is evident by comparing the NPGO index with indices of strength of the NPC [*Di Lorenzo et al.*, 2008] and the KOE [*Taguchi et al.*, 2007] inferred by taking the average meridional gradient of SSH in the NPC and KOE region respectively (Figure 1). Using satellite observations between 1993–2005 and simplified wind-forced ocean models, *Cummins and Freeland* [2007] also isolate the NPGO pattern in the SSHa (Figure 1), which they refer to as the "breathing mode", and link it to changes in the strength of the NPC. The NPGO spatial and temporal signature emerges also in the second mode of North Pacific SSTa [*Chhak et al.*, 2009], which has been previously referred to as the "Victoria Mode" [*Bond et al.*, 2003]. Dynamically, the NPGO is forced by the atmosphere [*Chhak et al.*, 2009] and is the oceanic expression of the North Pacific Oscillation (NPO)—the second dominant

[1]School of Earth and Atmospheric Sciences, Georgia Institute of Technology, Atlanta, Georgia, USA.
[2]Ocean Sciences, University of California, Santa Cruz, California, USA.
[3]International Pacific Research Center, University of Hawaii at Manoa, Honolulu, Hawaii, USA.
[4]Scripps Institution of Oceanography, University of California, San Diego, La Jolla, California, USA.
[5]Southwest Fisheries Science Center, NMFS, NOAA, Pacific Grove, California, USA.
[6]School of Marine Sciences, University of Maine, Orono, Maine, USA.
[7]Institute of Ocean Sciences, Fisheries and Oceans Canada, Sidney, British Columbia, Canada.
[8]JISAO, University of Washington, Seattle, Washington, USA.

0094-8276/09/2009GL038261

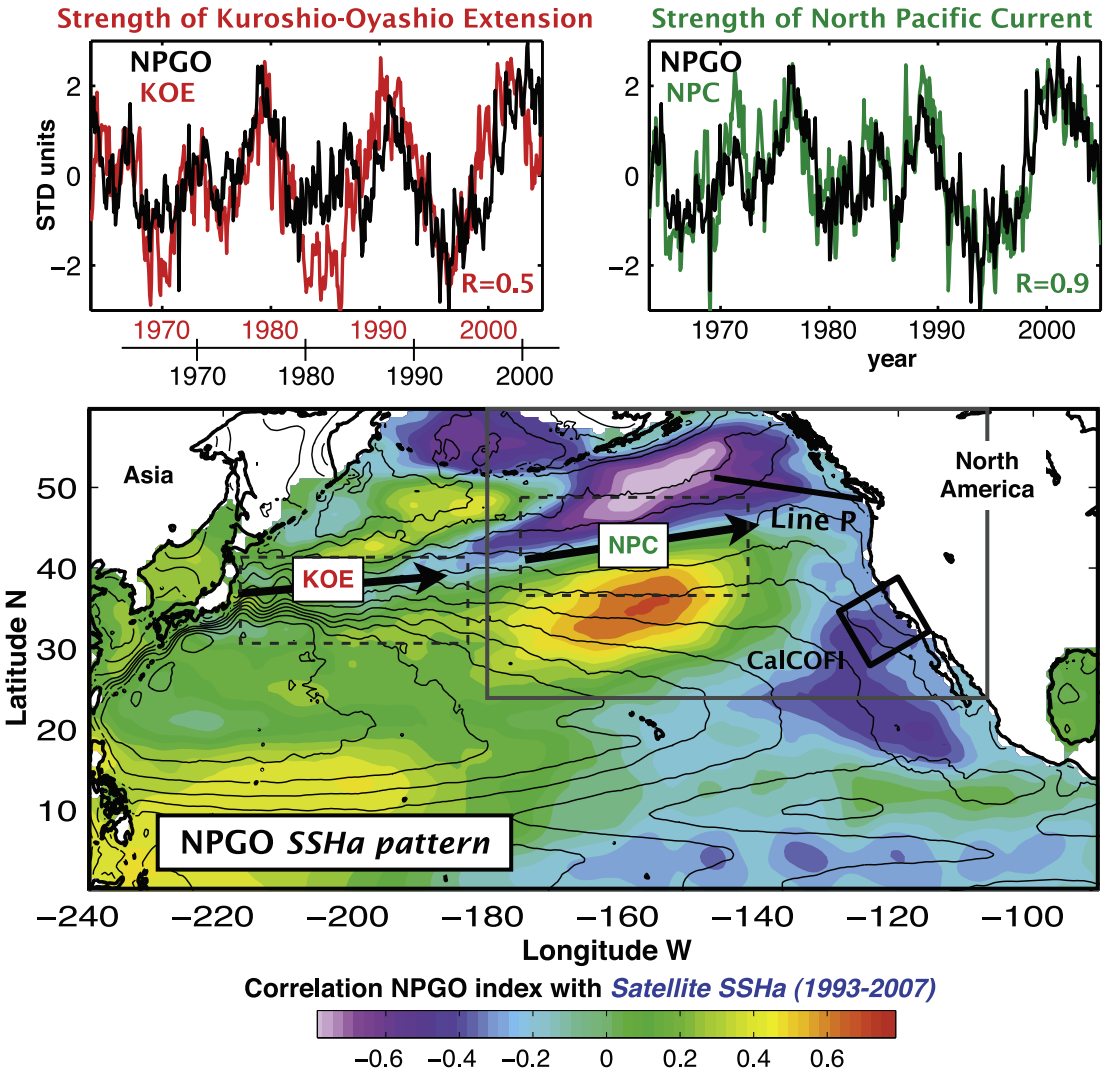

Figure 1. Temporal and spatial structure of the North Pacific Gyre Oscillation (NPGO). (top) Timeseries of NPGO index compared with indices that track the strength of the Kuroshio-Oyashio Extension (KOE, red curve) and North Pacific Current (NPC, green curve). The KOE index is from *Taguchi et al.* [2007] and lags the NPGO by 3 years. The NPC index is from *Di Lorenzo et al.* [2008] model data and is plotted with no time lag. The two indices are computed by taking the meridional gradient of SSH over the KOE and NPC regions respectively defined by the black arrows and gray dotted rectangle in Figure 1 (bottom). The indices are anomalies from their monthly means. (bottom) Correlation map between NPGO index and AVISO satellite SSHa (1993–2007; http://www.jason.oceanobs.com). The dark gray rectangle shows the spatial domain used to perform the regional physical-nutrient model hindcast from 1950–2004. Also shown are the locations of the long-term observations of nutrients and salinity from the CalCOFI program in the California Current and Line P in the Gulf of Alaska. Black contours are satellite/drifter-derived mean dynamic height [*Niiler et al.*, 2003].

pattern of sea level pressure variability in the North Pacific [*Linkin and Nigam*, 2008]. Because of the large-scale coherency of the NPGO spatial expressions (e.g., SSHa in Figure 1) between the CCS and the GoA, the NPGO index may serve as an indicator of low-frequency changes in the salinity and nutrients recorded along Line P.

[4] This paper aims to show that low-frequency variations of surface salinity and upper ocean nutrients along Line P are explained by the NPGO and are positively correlated with the corresponding CCS timeseries. This finding is also supported by numerical simulations conducted with a regional ocean circulation model coupled to a nutrient-phytoplankton-zooplankton-detritus (NPZD) ecosystem model. The leading modes of surface salinity and subsurface nutrient variability of the model are strongly correlated with the NPGO and exhibit a large-scale coherent structure that adequately predicts the observed in-phase relationship between the Alaskan Gyre and California Current timeseries.

2. Observational and Model Data

[5] We investigate the surface salinity and subsurface nutrients leading mode of variability using a high-resolution ocean circulation model of the northeast Pacific coupled to an NPZD ecosystem model. We use the Regional Ocean

Modeling System (ROMS) [*Shchepetkin and McWilliams*, 2005; *Haidvogel et al.*, 2008] in a nested configuration over the northeast Pacific region 180°W–110°W; 25°N–62°N. The model computational grid has a horizontal resolution of 1/5 of a degree with 30 vertical terrain-following layers. This type of model configuration is eddy-permitting and has been used in previous studies to successfully capture both the mean and long-term variability of the CCS [*Marchesiello et al.*, 2003; *Di Lorenzo et al.*, 2008]. The surface wind stresses and heat fluxes used to force the model are from the US National Center for Environmental Prediction (NCEP) [*Kistler et al.*, 2001] for the period 1950–2004. At the surface we use a corrected monthly climatology of heat and freshwater fluxes for temperature and salinity to avoid long-term drifts associated with errors in the NCEP surface fluxes [*Josey*, 2001]. This corrected flux climatology is estimated by saving the net surface fluxes of a 100 year spin-up run where the surface temperature and salinity are relaxed to their observed climatologies with a timescale $\approx$ 1 month. To account for the temporal variability in the heat flux for the hindcast integration 1950–2004, we add to the corrected monthly climatology a time-dependent relaxation to SST reanalysis [*Smith and Reynolds*, 2004] with a timescale $\approx$ 1 month. For the salinity surface boundary condition we only use the corrected monthly flux climatology with no surface relaxation and thereby assume that the dominant changes in salinity on periodicities larger than the seasonal cycle are only controlled by ocean advection. The ecosystem sub-model includes nutrient-phytoplankton-zooplankton-detritus (NPZD) and uses the same parameter settings as those of *Powell et al.* [2006]. The initial conditions along with monthly climatological open boundary conditions for nutrients are extracted from the nitrate (NO_3) field of the World Ocean Atlas available at http://www.nodc.noaa.gov. The other ecosystem components are set to constants both in the initial and open boundary conditions (phytoplankton = 0.08; zooplankton = 0.06; detritus = 0.04; units are μmol NO_3 m^{-3}) and evolve to equilibrium concentrations in the first 25 years (1950–1975) of the hindcast run.

[6] The observational and model timeseries presented in this study are monthly averaged anomalies, where the anomalies are computed by removing the long-term monthly means (1963–2004 for Line P and CalCOFI salinity data; 1984–2004 for CalCOFI nutrients and 1969–2004 for Line P nutrients). The analyses presented are insensitive to the reference period used to define the anomalies. From 1970 to 1984, the CalCOFI salinity timeseries has several data gaps that we fill with the Scripps Pier salinity timeseries located in the southern CCS. The Scripps Pier salinity is an excellent proxy of the CalCOFI salinity over the period 1963–2004 with correlations of R = 0.8 of the raw timeseries and R = 0.92 of the 5 year low-passed data. The merging of the two datasets is done by averaging the two signals when both are available and using the Scripps Pier data when CalCOFI is missing. Our analysis and comparisons focus on the period 1963–2004 when the model estimate of the oceanic variability is less affected by errors in the NCEP wind forcing, which are particularly evident between 1950–1963 [see *Di Lorenzo et al.*, 2005, Figure 4]. The first 25 years of the NPZD model integration are used as spin-up, therefore the model nutrient analysis focus on the period 1975–2004.

[7] The significance of the correlation coefficients is estimated from the Probability Distribution Functions (PDFs) of the correlation coefficient of two red-noise timeseries with the same autoregression coefficients as estimated from the original signals. The PDFs are computed numerically by generating 3000 realizations of the correlation coefficient of two random red-noise timeseries. The correlations are computed over the period 1963–2004 for the salinity data, 1984–2004 for the CalCOFI nutrients and 1969–2004 for the Line P nutrients excluding a period of time centered around 1985 when there is little to no nutrient data for Line P.

3. Salinity and Nutrient Variability

[8] The dominant spatial and temporal modes of variability for surface salinity and subsurface nutrients (150 m depth) from the ROMS-NPZD model are extracted by computing the first Empirical Orthogonal Function (EOF1, spatial pattern) and corresponding Principal Component (PC1, temporal evolution of EOF1) for each field.

3.1. Surface Salinity

[9] The EOF1 of model surface salinity (Figure 2b) is characterized by positive anomalies in the Alaskan Gyre and CCS regions, and negative anomalies in the subtropical gyre. To first order, the structure of the spatial anomalies resembles the distribution of the mean surface salinity (Figure 2a) but opposite in sign, with high salinity anomalies (low in the mean) over the Alaskan Gyre and CCS regions and fresher (saltier in the mean) water masses in the subtropics. However, the like signed anomalies in the GoA and CCS are separated by a weak, opposite signed signal between 130W–124W and at the coast from 41N–48N. Along the coast, this out-of-phase signal is a robust feature that is evident also in independent satellite chlorophyll-a analysis [*Thomas*, 2009] and marks the transitional boundary between two upwelling low-frequency regimes associated with the PDO north of $\sim$38N [*Chhak and Di Lorenzo*, 2007] and the NPGO south of $\sim$38N [*Di Lorenzo et al.*, 2008]. The temporal evolution of the first salinity mode (PC1) is significantly correlated with the NPGO index (R = 0.67; 99%). The observed salinity anomaly timeseries in the GoA (R = 0.4; 96%) and CCS (R = 0.56; 95%) are also strongly correlated with the NPGO index (Figure 2c). The correlations with the GoA salinity are higher (R = 0.6; 99%) before the period 1993–2004, when there is an offset in the phase of the last cycle. The correlation between the NPGO index and observed salinity timeseries is attributed to variance in the low frequencies. If we filter the timeseries with a 5 year low-pass the correlations reach a significant (>95%) maximum of R = 0.7 (CCS), R = 0.52 (GoA) and R = 0.8 (GoA without the 1993–2004 period).

[10] The EOF1 of the model adequately predicts the in-phase relationship between the GoA and CCS seen in the observations, and supports the existence of large-scale modes of surface salinity variability in the northeast Pacific. We also note that in the ROMS model hindcast configuration, surface salinity variations beyond the seasonal timescales are only controlled by changes in ocean advection and mixing. This suggests that the dynamics controlling low-frequency salinity fluctuations at Line P and in the

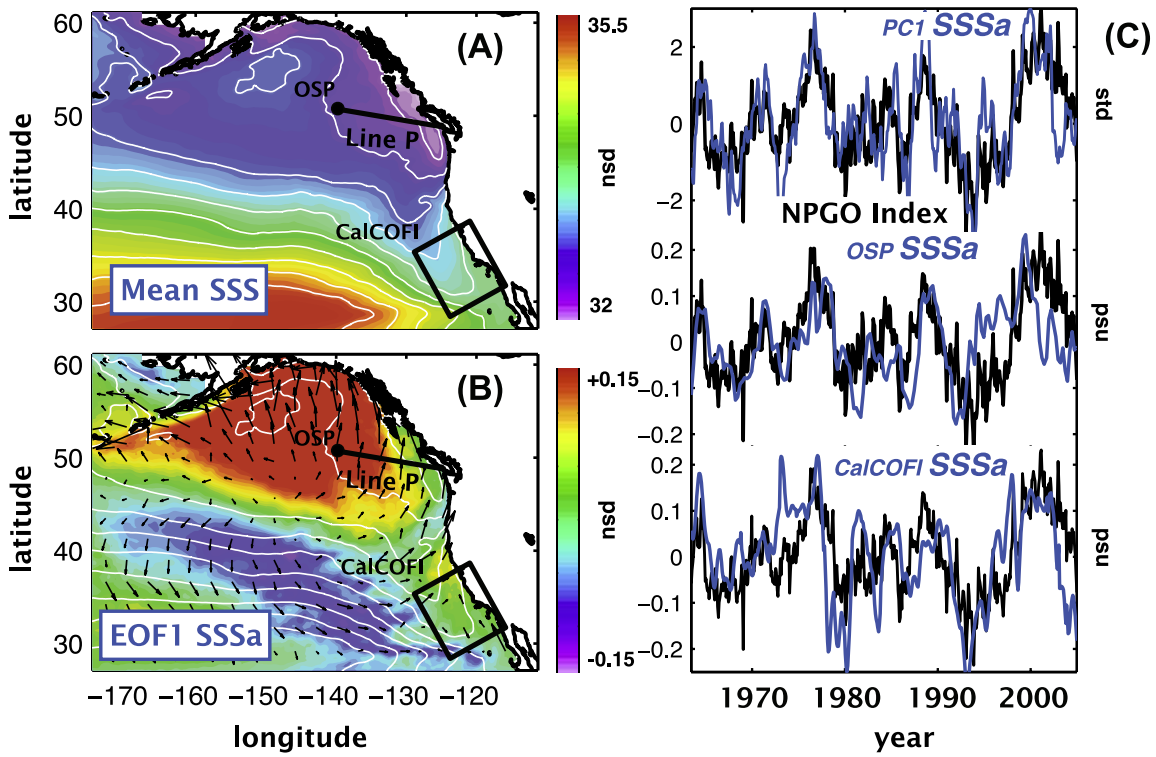

Figure 2. Temporal and spatial variability of surface salinity. (a) Mean surface salinity (SSS) from ROMS ocean model over the period 1950–2004. Units for salinity are in psu. (b) First mode of variability for model surface salinity anomaly (SSSa) inferred from EOF1. Black arrows in Figure 2b correspond to model surface currents anomalies during the positive phase of the NPGO. White contours mark the mean salinity distributions in both Figures 2a and 2b. (c) Timeseries of NPGO index (black) compared to PC1 of SSSa (R = 0.67, 99%), observed SSSa at ocean Station Papa (OSP) (R = 0.40, 96%) at the offshore end of Line P [*Crawford et al.*, 2007], and observed SSSa from CalCOFI program (R = 0.56, 99%). The PC1 of SSSa is normalized by its standard deviation, units are in standard deviations (std).

CalCOFI domain are not dependent on precipitation, evaporation or river runoff. A detailed analysis of the surface salinity budget for this model simulation [*Chhak et al.*, 2009] reveals that in the GoA the spatial and temporal patterns of salinity variability are determined by the displacement of the mean salinity gradients by anomalies in the zonal Ekman currents (black arrows shown in Figure 2b) and Ekman pumping anomalies associated with the NPGO atmospheric forcing. In contrast, in the CCS both the meridional and zonal components of anomalous Ekman currents, and coastal upwelling appear to be important [*Chhak et al.*, 2009].

3.2. Upper Ocean Nutrients

[11] Low-frequency fluctuations of nitrate in the upper ocean are strongly correlated with phosphate, silicate, salinity and oxygen in the GoA along Line P [*Wong et al.*, 2007; *Whitney et al.*, 2007] and in the CCS over the CalCOFI sampling domain [*Bograd et al.*, 2003]. In the model we characterize the nutrient variability using the nitrate field at 150m depth over the period 1975–2004 (the period 1950–1975 is used as spin-up for the NPZD model). At this depth model variations in nutrients are predominantly driven by changes in oceanic advection and therefore linked to the physical circulation rather than ecosystem processes. Mean nitrate patterns at 150m show elevated concentrations around the entire GoA and CCS basin margins (Figure 3a). The EOF1 of model nitrate variability at 150 m is characterized by positive anomalies along the entire North American boundary (Figure 3b). This spatial structure is very similar to the mean distribution of nitrate suggesting that EOF1 captures modulations in the magnitude of the mean nitrate distribution. The NPGO index is strongly correlated with the model nitrate PC1 (R = 0.65; 99%), and with Line P (R = 0.68; 99%) and CalCOFI observations (R = 0.51 95%) (Figure 3c). The 5 year low-pass timeseries reach a significant (>95%) maximum correlation with R = 0.86 (CalCOFI-CCS) and R = 0.82 (Line P-GoA). As in the salinity case, the EOF1 of the model adequately predicts the in-phase relationship between the GoA and CCS seen in the observations, and provides evidence of large-scale modes of nutrient variability in the northeast Pacific.

4. Summary and Discussions

[12] Long-term timeseries of upper ocean salinity and nutrients collected in the Alaskan Gyre along Line P exhibit significant low-frequency variations that are shown to be in phase with variations recorded in the California Current System by the California Cooperative Oceanic Fisheries Investigation (CalCOFI). We present evidence that these variations are both associated with the North Pacific Gyre Oscillation (NPGO)—a climate mode of variability that tracks changes in strength of the central and eastern branches of the North Pacific gyres and of the Kuroshio-

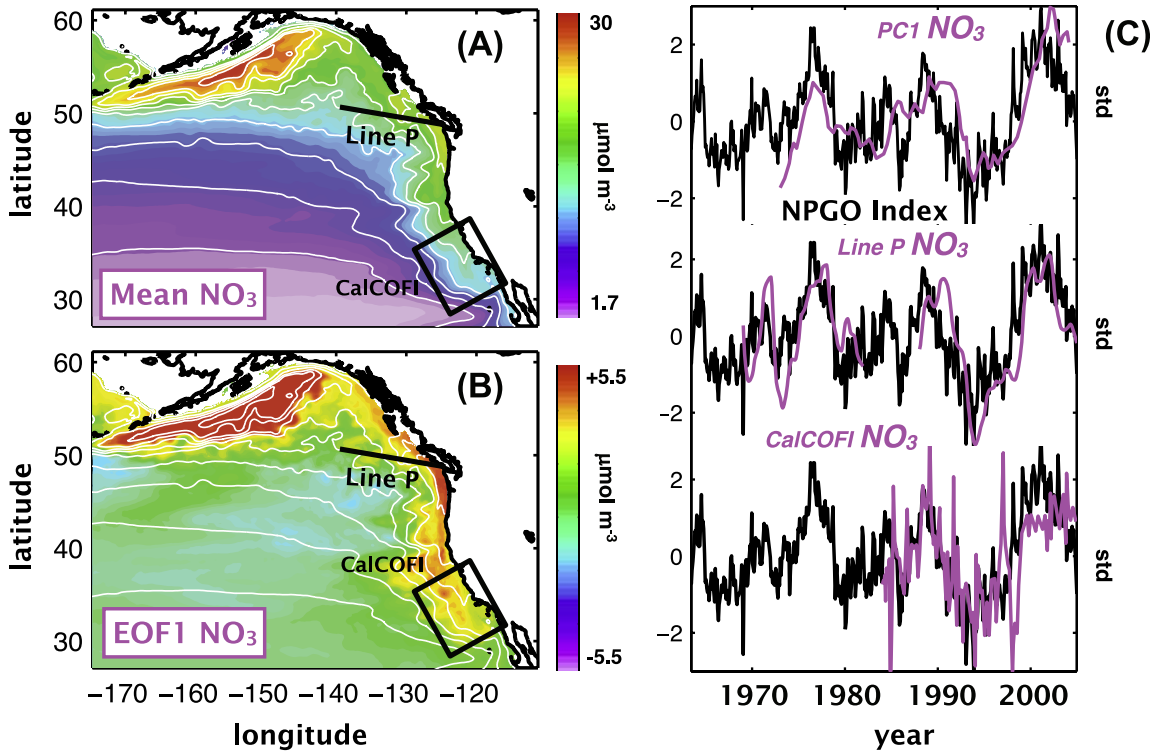

Figure 3. Temporal and spatial variability of subsurface nitrate (NO3). (a) Mean subsurface (150 m) NO3 from ROMS ocean model over the period 1975–2004. (b) First mode of variability for model subsurface (150 m) NO3 anomaly inferred from EOF1. White contours mark the mean NO3 distributions in Figures 3a and 3b. (c) Timeseries of NPGO index (black) compared to PC1 of NO3 (R = 0.65, 99%), observed mix layer NO3 at Line-P [*Peña and Varela*, 2007] (R = 0.68, 99%), and observed NO3 from CalCOFI program (R = 0.51, 95%). All timeseries are normalized by their standard deviations, units are in standard deviations (std).

Oyashio Extension (KOE). Even though the NPGO is the second dominant mode of variability of SSHa and SSTa in the northeast Pacific, it emerges as the leading mode of decadal variability for surface salinity and upper ocean nutrients. We reconstructed the spatial expressions of the salinity and nutrient modes over the northeast Pacific using a regional ocean model hindcast from 1963–2004. These modes exhibit a large-scale coherent pattern that adequately predict the in-phase relationship between the Alaskan Gyre and California Current datasets. The patterns of nutrient and salinity variability are distinct and similar to their respective mean distributions. The structure of the nutrient mode is characterized by higher values along the northeast Pacific boundary during the positive phase of the NPGO, while the dominant salinity mode exhibits positive salinity anomalies in the Alaskan gyre and California Current region, and negative anomalies in the subtropical gyre. The fact that it is fluctuations in the second mode of SSHa and SSTa variability that explain the dominant nutrients fluctuations has important consequences for our current understanding of bottom-up forcing and lower trophic ecosystem dynamics of the northeast Pacific.

[13] Our findings confirm that—similar to temperature and sea surface height—the salinity and nutrient fields exhibit coherent patterns of variability that are connected with basin-scale climate fluctuations. The fact that large-amplitude, low-frequency fluctuations in biologically relevant properties in the northeast Pacific are spatially phase-locked and correlated with a measurable climate index (the NPGO) open new avenues for exploring and predicting the effects of long-term climate change on marine ecosystem dynamics in the entire northeast Pacific and beyond. Ongoing work is exploring the utility of the NPGO as an additional predictive index of ecosystem change in the Pacific basin.

[14] This study also suggests that the first two modes of oceanic low-frequency variability of the central/eastern North Pacific (e.g., PDO and NPGO) are equally important and must be considered together when quantifying the low-frequency oceanic variability.

[15] **Acknowledgments.** We acknowledge the support of the NSF OCE-0550266, GLOBEC-0606575, OCE-0452654, OCE-0452692, CCS-LTER, GLOBEC OCE-0815280, OCE05-50233, OCE-0815051, OCE-0535386, OCE-0647815, OCE-0452692, NASA NNG05GC98G, Office of Science (BER), DOE DE-FG02-07ER64469 and JAMSTEC.

References

Bograd, S. J., et al. (2003), CalCOFI: A half century of physical, chemical, and biological research in the California Current System, *Deep Sea Res., Part II*, *50*(14–16), 2349–2353.

Bond, N. A., J. E. Overland, M. Spillane, and P. Stabeno (2003), Recent shifts in the state of the North Pacific, *Geophys. Res. Lett.*, *30*(23), 2183, doi:10.1029/2003GL018597.

Ceballos, L. I., et al. (2009), North Pacific Gyre Oscillation synchronizes climate fluctuations in the eastern and western boundary systems, *J. Clim.*, doi:10.1175/2009JCLI2848.1, in press.

Chhak, K., and E. Di Lorenzo (2007), Decadal variations in the California Current upwelling cells, *Geophys. Res. Lett.*, *34*, L14604, doi:10.1029/2007GL030203.

Chhak, K., et al. (2009), Forcing of low-frequency ocean variability in the northeast Pacific, *J. Clim.*, *22*(5), 1255–1276.

Crawford, W., et al. (2007), Line P ocean temperature and salinity, 1956–2005, *Prog. Oceanogr.*, *75*(2), 161–178.

Cummins, P. F., and H. J. Freeland (2007), Variability of the North Pacific current and its bifurcation, *Prog. Oceanogr.*, *75*(2), 253–265.

Di Lorenzo, E., et al. (2005), The warming of the California Current: Dynamics and ecosystem implications, *J. Phys. Oceanogr.*, *35*(3), 336–362.

Di Lorenzo, E., et al. (2008), North Pacific Gyre Oscillation links ocean climate and ecosystem change, *Geophys. Res. Lett.*, *35*, L08607, doi:10.1029/2007GL032838.

Freeland, H. (2007), A short history of ocean station papa and Line P, *Prog. Oceanogr.*, *75*(2), 120–125.

Haidvogel, D. B., et al. (2008), Ocean forecasting in terrain-following coordinates: Formulation and skill assessment of the Regional Ocean Modeling System, *J. Comput. Phys.*, *227*(7), 3595–3624.

Josey, S. A. (2001), A comparison of ECMWF, NCEP-NCAR, and SOC surface heat fluxes with the moored buoy measurements in the subduction region of the northeast Atlantic, *J. Clim.*, *14*(8), 1780–1789.

Linkin, M. E., and S. Nigam (2008), The North Pacific Oscillation–west Pacific teleconnection pattern: Mature-phase structure and winter impacts, *J. Clim.*, *21*(9), 1979–1997.

Kistler, R., et al. (2001), The NCEP-NCAR 50-year reanalysis: Monthly means CD-ROM and documentation, *Bull. Am. Meteorol. Soc.*, *82*(2), 247–267.

Mantua, N. J., et al. (1997), A Pacific interdecadal climate oscillation with impacts on salmon production, *Bull. Am. Meteorol. Soc.*, *78*(6), 1069–1079.

Marchesiello, P., et al. (2003), Equilibrium structure and dynamics of the California Current System, *J. Phys. Oceanogr.*, *33*(4), 753–783.

McGowan, J. A., et al. (2003), The biological response to the 1977 regime shift in the California Current, *Deep Sea Res., Part II*, *50*(14–16), 2567–2582.

Niiler, P. P., N. A. Maximenko, and J. C. McWilliams (2003), Dynamically balanced absolute sea level of the global ocean derived from near-surface velocity observations, *Geophys. Res. Lett.*, *30*(22), 2164, doi:10.1029/2003GL018628.

Peña, M. A., and S. J. Bograd (2007), Time series of the northeast Pacific, *Prog. Oceanogr.*, *75*(2), 115–119.

Peña, M. A., and D. E. Varela (2007), Seasonal and interannual variability in phytoplankton and nutrient dynamics along Line P in the NE subarctic Pacific, *Prog. Oceanogr.*, *75*(2), 200–222.

Powell, T. M., C. V. W. Lewis, E. N. Curchitser, D. B. Haidvogel, A. J. Hermann, and E. L. Dobbins (2006), Results from a three-dimensional, nested biological-physical model of the California Current System and comparisons with statistics from satellite imagery, *J. Geophys. Res.*, *111*, C07018, doi:10.1029/2004JC002506.

Shchepetkin, A. F., and J. C. McWilliams (2005), The regional oceanic modeling system (ROMS): A split-explicit, free-surface, topography-following-coordinate oceanic model, *Ocean Modell.*, *9*(4), 347–404.

Smith, T. M., and R. W. Reynolds (2004), Improved extended reconstruction of SST (1854–1997), *J. Clim.*, *17*(12), 2466–2477.

Taguchi, B., et al. (2007), Decadal variability of the Kuroshio Extension: Observations and an eddy-resolving model hindcast, *J. Clim.*, *20*(11), 2357–2377.

Thomas, A. C. (2009), Interannual variability in chlorophyll concentrations in the Humboldt and California Current Systems, *Prog. Oceanogr.*, in press.

Whitney, F. A., et al. (2007), Persistently declining oxygen levels in the interior waters of the eastern subarctic Pacific, *Prog. Oceanogr.*, *75*(2), 179–199.

Wong, C. S., et al. (2007), Variations in nutrients, carbon and other hydrographic parameters related to the 1976/77 and 1988/89 regime shifts in the sub-arctic northeast Pacific, *Prog. Oceanogr.*, *75*(2), 326–342.

S. J. Bograd, Southwest Fisheries Science Center, NMFS, NOAA, 1352 Lighthouse Avenue, Pacific Grove, CA 93950-2097, USA.

A. Bracco and E. Di Lorenzo, School of Earth and Atmospheric Sciences, Georgia Institute of Technology, 311 Ferst Drive, Atlanta, GA 30332, USA. (edl@gatech.edu)

W. R. Crawford and A. Peña, Institute of Ocean Sciences, Fisheries and Oceans Canada, 9860 West Saanich Road, Sidney, BC V8L 4B2, Canada

J. Fiechter and A. M. Moore, Ocean Sciences, University of California, 1156 High Street, Santa Cruz, CA 95064, USA.

P. J. S. Franks and A. J. Miller, Scripps Institution of Oceanography, University of California, San Diego, 9500 Gilman Drive, La Jolla, CA 92093-0218, USA.

A. J. Hermann, JISAO, University of Washington, 7600 Sandy Point Way NE, Seattle, WA 98115, USA.

N. Schneider, International Pacific Research Center, University of Hawaii at Manoa, 1680 East-West Road, Honolulu, HI 96822, USA.

A. C. Thomas, School of Marine Sciences, University of Maine, 5706 Aubert Hall, Orono, ME 04469-5706, USA.